Radiated seismic energy and earthquake source duration variations from teleseismic source time functions for shallow subduction zone thrust earthquakes

S. L. Bilek
Department of Earth and Environmental Science, New Mexico Institute of Mining and Technology, Socorro, New Mexico, USA

T. Lay
Department of Earth Sciences, University of California, Santa Cruz, California, USA

L. J. Ruff
Department of Geological Sciences, University of Michigan, Ann Arbor, Michigan, USA

Received 24 February 2004; revised 29 June 2004; accepted 19 July 2004; published 25 September 2004.

[1] Earthquake source time functions deconvolved from teleseismic broadband *P* wave recordings are used to examine rupture variations for 417 underthrusting earthquakes located on the interplate interface in circum-Pacific subduction zones. Moment-scaled duration of significant moment release varies with depth, with longer-duration events occurring in the shallowest 20 km of the megathrusts. The source time functions are also used to estimate radiated seismic energy. Two estimates are obtained: a simple scaled triangle substitution for the moment release history provides a minimum estimate, while integration of the time function shape provides an estimate limited only by the bandwidth of the teleseismic deconvolutions. While these energy calculations underestimate total energy, they enable systematic comparisons of rupture process within and between subduction zones. We do not find significant depth dependence for radiated energy overall, but some regions do show mild trends of increasing energy/seismic moment ratios (E/M_o) with increasing source depth that correspond to rupture duration variations in those regions. The observations of longer rupture duration at shallow depth with moderate E/M_o may be due to heterogeneous friction and structural features on the shallow plate interface. *INDEX TERMS:* 7215 Seismology: Earthquake parameters; 7230 Seismology: Seismicity and seismotectonics; 8164 Tectonophysics: Stresses—crust and lithosphere; *KEYWORDS:* radiated energy, shallow subduction, source parameters

Citation: Bilek, S. L., T. Lay, and L. J. Ruff (2004), Radiated seismic energy and earthquake source duration variations from teleseismic source time functions for shallow subduction zone thrust earthquakes, *J. Geophys. Res.*, *109*, B09308, doi:10.1029/2004JB003039.

1. Introduction

[2] Subduction zones in the circum-Pacific host approximately 70% of the world's earthquakes. The majority of events involve thrusting on the interplate megathrust, which is seismically coupled from depths of a few kilometers to 30–50 km. Earthquakes within the shallow seismogenic environment of subduction zones exhibit diverse rupture behavior. This includes a wide range of seismic magnitudes (e.g., from microearthquakes to great events such as M_w = 9.5 1960 Chile and M_w = 9.2 1964 Alaska) and complexity variations from very simple rupture histories to very complex multiple events. This variability also extends to a range of timescales for moment release, including typical earthquake rupture times, slower earthquakes that may produce large tsunamis, and very slow creep events not detected seismically. Systematic investigation of seismic source parameters is an important approach to understanding the variable nature of subduction zone earthquakes.

[3] Variability in subduction zone physical characteristics contributes to regional variations in typical shallow subduction zone seismicity [*Ruff and Kanamori*, 1980; *Lay et al.*, 1982]. *Zhang and Schwartz* [1992] find correlations between seismic moment release and subduction zone convergence rate and sediment thickness. Within the Japan subduction zone, along strike and down-dip variations in large earthquake rupture have been related to variations of the incoming plate bathymetric structure [*Tanioka et al.*, 1996]. Other studies examine stress drop and source dura-

0148-0227/04/2004JB003039$09.00

tion variations for shallow and deep earthquakes, invoking a number of possibilities (such as sediment subduction, thermal structure, hydrologic effects, and plate structure) for producing the earthquake rupture variability [*Ekström and Engdahl*, 1989; *Vidale and Houston*, 1993; *Bos et al.*, 1998; *Houston et al.*, 1998; *Bilek and Lay*, 1999, 2000]. Anomalously long-duration events of moderate size ($\sim M$ 6.0) have been found at depths <15 km in several regions [*Bilek and Lay*, 1999, 2000].

[4] Tsunami earthquakes as defined by *Kanamori* [1972] are tsunamigenic events at shallow depths that typically have long rupture durations and seismic moments estimated from 100 s period waves significantly larger than those determined from higher frequency waves. One early explanation for the large tsunami and slow deformation involves rupture on steeply dipping splay faults within the accretionary wedge [*Fukao*, 1979]. Other explanations invoke earthquake rupture along the megathrust at the base of the accretionary wedge, large displacements in weaker materials at very shallow depths, or heterogeneous distribution of frictional conditions in the shallowest extent of the subduction zones [*Okal*, 1988; *Pelayo and Wiens*, 1992; *Kanamori and Kikuchi*, 1993; *Satake*, 1994; *Tanioka and Satake*, 1996; *Satake and Tanioka*, 1999; *Polet and Kanamori*, 2000; *Seno*, 2002; *Bilek and Lay*, 2002].

[5] Slow creep events, usually involving significant postseismic slip on the megathrust over days to years following the coseismic slip of normal interplate thrust events, are being recognized as more subduction zones are monitored with high- quality geodetic networks. Early observations focused on the northeastern coast of Japan, particularly following earthquakes in 1992 [*Kawasaki et al.*, 1995] and 1994 [*Heki et al.*, 1997; *Heki and Tamura*, 1997]. Other earthquakes, including events in Mexico, Peru, and Chile, have been followed by these slow slip transients, yet explanations for their occurrence and regional variability are still debated [*Lowry et al.*, 2001; *Melbourne et al.*, 2002]. Interseismic creep at depths below the seismogenic interface is also now being resolved. Silent creep at depths below the locked seismogenic portion of the Cascadia megathrust has been observed and modeled using GPS data in the Pacific Northwest [*Dragert et al.*, 2001; *Miller et al.*, 2002; *McGuire and Segall*, 2003]. Triggers for these transients may be other earthquakes in the region, or perhaps controlled by conditional frictional conditions along the fault [*McGuire and Segall*, 2003].

[6] Much of our understanding of interplate thrust earthquakes comes from routine analysis to determine focal mechanism, centroid depth, and seismic moment. Some efforts are made to routinely estimate the source moment rate function, describing the time history of faulting and slip. Radiated seismic energy is another important seismological parameter for understanding earthquake physics. Seismic wave energy can be related to strains during large earthquakes and is used for examining apparent stress and seismic efficiency for earthquakes [*McGarr*, 1999]. Radiated energy has been estimated for many earthquakes but is still poorly constrained. Earlier studies show significant variability and large discrepancies (up to an order of magnitude) between estimates made with regional and teleseismic data [*Kikuchi and Fukao*, 1988; *Choy and Boatwright*, 1995; *Newman and Okal*, 1998; *Singh and Ordaz*, 1994; *Mayeda and Walter*, 1996; *Pérez-Campos and Beroza*, 2001]. More recent attempts have reconciled many of these differences between teleseismic and regional estimates by accounting for attenuation and site effects [*Venkataraman et al.*, 2002; *Pérez-Campos et al.*, 2003] and source directivity [*Venkataraman and Kanamori*, 2004a].

[7] There are studies indicating that shallow subduction zone earthquake energy estimates may vary for events classified as tsunami earthquakes relative to more typical subduction zone events. *Newman and Okal* [1998] find that recent tsunami earthquakes stand out from the general population of earthquakes, suggesting that their lower energy measures relative to seismic moment (E/M_o) can be used as a near real time discriminant for tsunami earthquakes. *Polet and Kanamori* [2000] also describe tsunami earthquakes as low energy relative to seismic moment, in contrast to typical large subduction zone earthquakes.

[8] This study uses a large data set of recent shallow ($\leq$60 km depth) interplate thrusting earthquakes from 14 circum-Pacific subduction zones to examine variability in earthquake source parameters using teleseismic source time functions determined from high quality broadband data. This global catalog of teleseismic source time functions provides measures of source duration as well as estimates of rupture complexity for many earthquakes in each subduction zone, allowing global and regional trends to be examined. We also use the time functions to estimate the radiated seismic energy from each earthquake, using two different methods that incorporate various information about the source time function shapes.

[9] Radiated energy can be calculated either from source time functions [e.g., *Vassiliou and Kanamori*, 1982] or by squaring, integrating and scaling seismic ground velocity recordings [e.g., *Winslow and Ruff*, 1999]. Calculating energy from the source time functions has an advantage, as the propagation effects are already explicitly removed from the time function [*Vassiliou and Kanamori*, 1982; *Kikuchi and Fukao*, 1988; *Kanamori*, 1994]. However, teleseismically derived estimates of the source time functions tend to be band limited and affected by deconvolution noise, which will reduce energy estimates in comparison with near field estimates. We recognize that our energy estimates will be reduced in this way, however the results presented here provide a large data set of energy estimates for shallow subduction zone thrust events computed in a consistent manner. Because of this consistency, we explore variations in energy release within individual subduction zones as well as between regions, seeking gross trends in the data despite the limitations of such energy estimates. We also estimate E/M_o for a catalog of historical tsunami earthquakes with published source time functions for comparison with our global subduction zone thrusting earthquake catalog. We find that energy radiated during tsunami earthquakes is lower than other shallow subduction zone events.

2. Methods

2.1. Data Selection

[10] Shallow seismicity in circum-Pacific subduction zones includes not only interplate thrust events but also intraslab, upper plate, and accretionary wedge events. As the goal of this study is to examine variations in megathrust

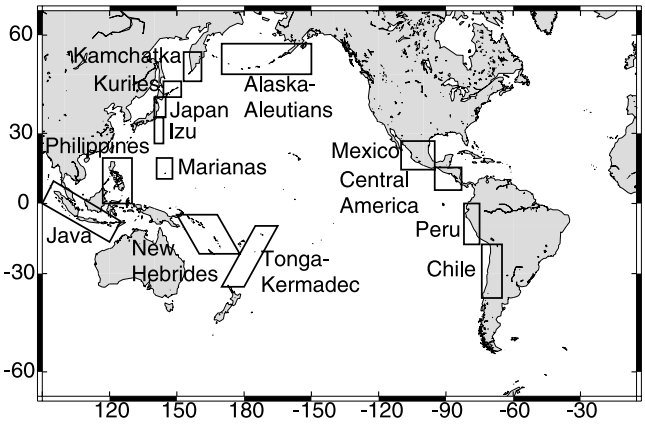

Figure 1. Map of subduction zones sampled in the combined source time function catalog. Boxes outline earthquake locations for each region.

earthquakes, criteria for event selection include appropriateness of focal mechanisms for the particular region (events identified as thrust by the moment tensor in the Harvard Centroid Moment Tensor catalog http://www.seismology.harvard.edu/CMTsearch.html), location near the interplate contact, earthquake magnitude (M_w 5.5–7.5), availability of station recordings over a wide range of azimuths, and data quality [*Bilek and Lay*, 2000]. Data for over 1000 earthquakes were examined, with many being eliminated due to low data quality, low signal to noise, or inability to determine a low misfit source time function. A small number of earthquakes at the smaller magnitude end of the range (5.5–5.9) are included because of the atypically good data quality for these events. Criteria for focal mechanism and source depth selection (see *Bilek and Lay* [2000] for details) used here are similar to those used in earlier studies of subduction zone earthquake variability [*Peterson and Seno*, 1984; *Pacheco et al.*, 1993; *Tichelaar and Ruff*, 1991; *Zhang and Schwartz*, 1992; *Tichelaar and Ruff*, 1993]. These earthquakes are located within close proximity to the main thrust zone of interest and have a faulting mechanism (from the Harvard CMT) with a strike, dip, and rake consistent with underthrusting of the subducting plate. Typically, these events have a strike within 20–30° of the local strike of the trench, a dip <30–35° and a rake of 90° ± 30°. Figure 1 shows the subduction zones used for this study. The event catalog consists of 345 source time functions produced as described below [*Bilek and Lay*, 1999, 2000] as well as 72 distinct source time functions provided by the MichSeis catalog (http://www.geo.lsa.umich.edu/SeismoObs/STF.html) which met the criteria above [*Tanioka and Ruff*, 1997].

2.2. Deconvolution of Source Time Function

[11] In order to determine accurate source time functions and depths for earthquakes not in the MichSeis catalog, all available teleseismic vertical component broadband recordings from the IRIS Data Management Center are considered, with time windows appropriate for the direct *P* phase and the associated depth phases (*pP*, *sP*) needed for accurate source depth determination. A multistation deconvolution method is used to determine the source time function that represents the time history of seismic moment release from the source [*Ruff and Kanamori*, 1983; *Ruff and Miller*, 1994]. The deconvolution method is based on computing synthetic *P* wave Green's functions for each event using the best double couple of the Harvard CMT solution for a model with a water layer over a uniform half-space with a *P* wave velocity of 6.0 km/s. Attenuation is corrected for using a frequency-independent $t^* = 1$ s. Observed *P* waves are deconvolved by Green functions generated for a range of 15–25 point source depths, obtaining source time functions for each trial depth. The depth at which the deconvolution minimizes the misfit between the data and synthetic seismograms is the optimal value used for the earthquake. While simultaneous inversion for a revised focal mechanism may reduce some uncertainties, it is not viable for most of these events given the limitations of the available *P* wave data. In general, trade-offs between source mechanism and either source depth or source time function are not too severe for shallow thrusting events, and the CMT solutions are probably fairly robust for most of our events.

[12] The processing results for two earthquakes from the Alaska-Aleutian Islands region are shown in Figure 2. For these events, 8 to 10 well-distributed *P* wave recordings are used in the deconvolution to ensure a diversity of wave shapes and corresponding Green's functions that reduces the severe trade-offs between depth and source time function

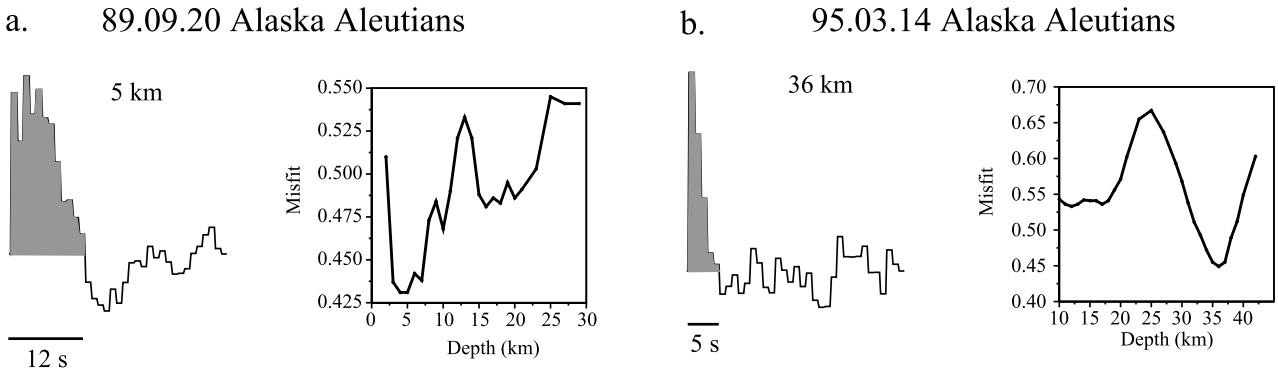

Figure 2. Source time functions for two earthquakes in the Alaska-Aleutian subduction zone. Inset graphs show range of depths used for the deconvolutions, with corresponding misfit. Optimal depth is chosen at the lowest misfit with the data. The source time function shown is for the optimal depth (indicated above). Duration of main pulse (shaded) is shown below each time function.

for isolated data or data from a narrow range of azimuths. From the deconvolution procedure, performed for 24 depths for the 1989 event and 28 depths for the 1995 event, we find an optimal depth of 5 km for the 1989 event and 36 km for the 1995 event based on the minimum in the misfit curves. The source time functions have initial pulse widths of 12 s and 5 s for the 1989 and 1995 events, respectively, with both source time functions containing low-amplitude oscillations later in the time functions. The latter oscillations are highly variable, and represent instabilities caused by accumulating inaccuracies in the Green functions with lapse time into the signals. As the two earthquakes are similar in magnitude, location, and mechanism, the main difference between the events is the source depth and source duration. The 1989 event has a shallower depth and a much longer duration than the deeper 1995 event. This trend of decreasing source duration with increasing depth is a consistent observation in the subduction zones in this study, and this is not attributable to depth-dependent biases in the focal mechanisms or the Green functions.

[13] There are several difficulties intrinsic to estimating source duration. Inaccuracies are associated with amplitude oscillations in the deconvolution, negative overshoot after the first pulse possibly due to error in Green functions, spatial finiteness of the source, uncertainty in focal mechanism, and use of simplified velocity model [e.g., *Bilek and Lay*, 2000]. It is very difficult to quantify uncertainty in the duration estimates. However, every earthquake time function we obtain does contain a primary pulse of moment rate in the early part of the signal that accounts well for the predominant features of the teleseismic P waves. Later, high variance portions of the time function generally do not account for coherent features in the signals, so we base our duration estimates on the primary pulse(s) in the time function.

[14] Consistent measurements for the width of the primary pulses in the source time functions are achieved by defining the end as the lag time at which the pulse returns to a baseline level. Error estimates determined for duration subjectively reflect the difficulties in measuring the time function duration and range between $\pm 0.5-2$ s. Depth determination is also difficult in some cases when double or multiple minima in the misfit curves occur, with error estimates ranging between $\pm 2-5$ km. For these cases, we examine the source time function produced for each depth, and choose the depth which yields the simplest time function, with most of the moment release concentrated early in the signal [*Christensen and Ruff*, 1985]. For earthquakes in the MichSeis catalog, we use the duration and depth values listed in the online catalog [*Tanioka and Ruff*, 1997]. Similar criteria have been used for these solutions.

[15] There are several key trade-offs in determining source duration and depth estimates. Source time function duration and depth have particularly strong trade-offs for individual stations [*Christensen and Ruff*, 1985]; however, by performing simultaneous deconvolution for many well-distributed stations, separation of these parameters is greatly improved. Additionally, there are trade-offs between velocity model and source depth. Our choice of a half-space velocity of 6.0 km/s undoubtedly produces bias in the duration and depth estimates. Tests using different average velocities show that an approximately 10% change in velocity gives a corresponding 8–12% change in source depth, in this case a 3–4 km change. Given the likelihood of low velocities being present in the sedimentary wedge above the thrust plane, we probably systematically overestimate true depths by several kilometers, particularly for the shallowest events. Using the 6.0 km/s velocity model, our depth estimates tend to be shallower than those in the CMT catalog, partly due to the higher average crustal and upper mantle velocity of the Preliminary Reference Earth Model (PREM) [*Dziewonski and Anderson*, 1981] structure used in the CMT inversion (for those CMT solutions not constrained to be 15 or 33 km depth). The velocity model also affects depth phase reflection coefficients and details of the Green's functions. However, given our ignorance of the detailed three-dimensional shallow structure in each subduction zone, we use a simple half-space model and rely on multiple station sampling to average out bias. Future work will incorporate more detailed velocity structures where available.

[16] Using a fixed focal mechanism is another source of possible error in the depth determinations, but tests of the effects of focal mechanism uncertainty indicate that the depth estimates are not particularly sensitive to small focal mechanism changes for shallow dipping thrust events and azimuthally distributed teleseismic wave signals. Depth errors of plus or minus a few kilometers reflect these sources of error. The point source assumption explicit in the simultaneous deconvolutions clearly results in some averaging of spatial finiteness effects that may bias the source duration estimates. Our procedure for estimation of source duration assumes a simple rupture process that yields negligible directivity effect. As most of our events are of moderate size, and the deconvolution process emphasizes wave periods longer than 1 or 2 s, the directivity effects in teleseismic *P* waves are likely to be below the resolution of these measurements in almost all cases. The good fit of the point source synthetics to the observations found in each case gives direct support for this assertion. The residual waveform mismatch error varies somewhat but not in a fashion simply linked to the shape of the source time functions or the event moment.

[17] The MichSeis catalog events extend our coverage for larger magnitudes. Comparison of earthquakes in common between the two subset catalogs shows that the MichSeis catalog durations tend to be ~ 2 s longer than the source time functions we obtain separately. Most of the difference appears to be related to differences in preferred centroid depths of on the order of 5–10 km. In many of those cases, there are several low misfit depths within a 5–8 km range. For the common events, using the depths listed in the MichSeis catalog gave comparable duration estimates for our separate deconvolutions. In the cases where these parameters differed significantly (as noted by *Houston* [2001]), modeling differences were apparent (e.g., the MichSeis catalog uses a focal mechanism found by inversion that is significantly different from the Harvard CMT mechanisms used in the routine processing described by *Bilek and Lay* [1999, 2000]).

[18] Rupture duration is generally found to be proportional to the cube root of seismic moment, M_o [*Kanamori and Anderson*, 1975; *Houston et al.*, 1998; *Campus and Das*, 2000]. Each duration estimate is divided by the cube root of the estimated earthquake M_o from the Harvard CMT

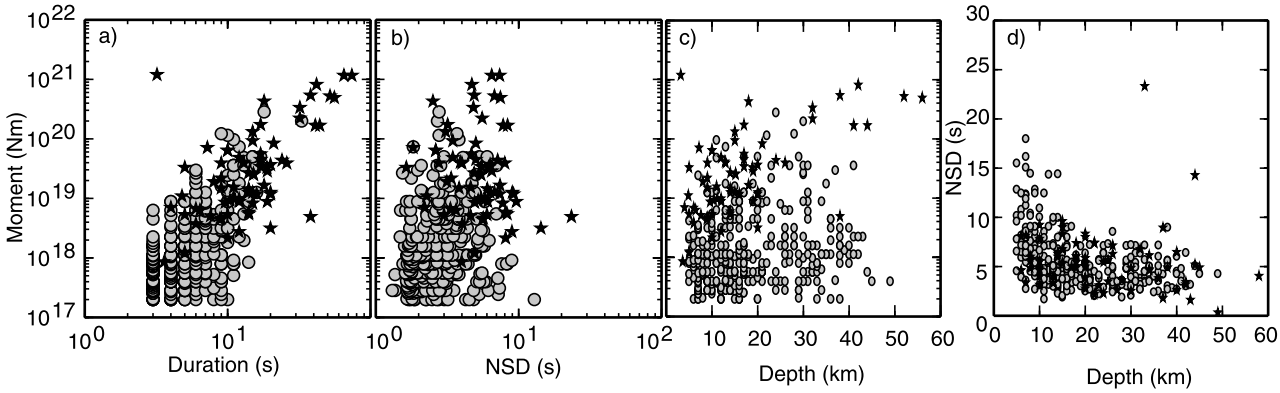

Figure 3. Source duration, seismic moment, and centroid depth for all 417 earthquakes in the combined catalog. Stars indicate earthquakes from the MichSeis catalog. (a) Duration as measured from the source time functions compared with seismic moment from the Harvard CMT catalog, showing the systematic $\sim$1/3 scaling with moment. (b) Moment-normalized duration (NSD) does not show a trend with moment. (c) Seismic moment versus centroid depth, showing lack of any trend. (d) Moment-normalized duration as a function of centroid depth, showing anomalously long duration at shallow depth.

catalog, normalized to a moment magnitude (M_w) 6.0 event. A typical rupture duration for an event of this size is about 3 s. The CMT moments are used for scaling rather than the moments determined from the deconvolution process, as the CMT moments are more stable estimates because they are derived from large numbers of long-period data. The deconvolution moments tend to underpredict the CMT values, in part due to the velocity model used, and possibly due to omission of later low-amplitude energy release. The difference in source depth estimate may also play a role. The unscaled durations show a clear increase with increasing M_o (Figure 3a). The moment normalization removes the effect of increasing duration with increasing moment (Figure 3b). This data set shows no systematic relationship between source depth and seismic moment (Figure 3c).

3. Duration Comparisons

[19] Normalized earthquake source duration variations with depth are summarized in Figure 3d for all 417 events in the data set. This augments the data sets previous presented by *Bilek and Lay* [1999, 2000], adding 63 observations for western Pacific and southwest Pacific subduction zones as well as the additional events from the MichSeis catalog. There is a general trend of decreasing source duration with increasing depth in the upper 20 km apparent when all subduction zones are plotted together. This can also be characterized as an increase in variability of source duration for depths <20 km. Scatter in the data set likely results from variations between subduction zones and velocity model errors.

[20] Examining normalized source duration measurements as a function of centroid depth for each of the 14 subduction zones separately reveals some regional patterns (Figure 4). All data are plotted at the same scale for ease of comparison. Some variation exists between regions, but the overall pattern of decreasing source duration with increasing depth is evident in most regions sampled. A few zones, such as the Marianas and Java lack sufficient range of depth to detect any trend. In most regions, shallow seismicity begins at depths <10 km, with the shallowest region having most of the anomalously long-duration events. In some cases, the patterns appear to have a change in the duration-depth behavior, from a rapid decrease with increasing depth to a much smaller change with depth at some depth between 10 and 20 km (i.e., Alaska, Kuriles). Only a couple of events deeper than 20 km stand out as having anomalously long ruptures. A couple of events also appear to be deeper than the normal interplate activity and these may be intraplate compressional events not distinguished by their focal mechanisms.

[21] Comparisons of simple parameterizations of the depth-dependent durations with various subduction zone parameters do not illuminate any clear regional behavior. Regional variations in maximum earthquake duration, as well as a ratio of duration for events $\leq$15 km deep to events >15 km deep, were compared with estimates for regional averages of convergence rate, plate age, plate dip [*Jarrard*, 1986; *von Huene and Scholl*, 1991], moment release depths [*Zhang and Schwartz*, 1992], sediment thickness [*von Huene and Scholl*, 1991], and sediment lithologies [*Rea and Ruff*, 1996]. There is no evident correlation between these subduction zone parameters and either maximum duration or the duration ratio parameterization (details are given by *Bilek* [2001]). While any systematic regional variations in the source time function durations may not be captured in the gross parameterizations of the entire subduction zone, other studies have also found little correlation between these subduction zone parameters and coupling or other earthquake patterns [*Pacheco et al.*, 1993; *Rea and Ruff*, 1996].

4. Energy Estimates

[22] Seismic energy estimates tend to have great variability as they depend strongly on bandwidth and fidelity of the source time function determinations. We provide a conservative set of estimates using a simple parameterized form of the source time functions and a more accurate set of estimates based on the full source time functions.

4.1. Triangle Substitution

[23] The large catalog of source time functions is used to estimate radiated seismic energy for subduction zone

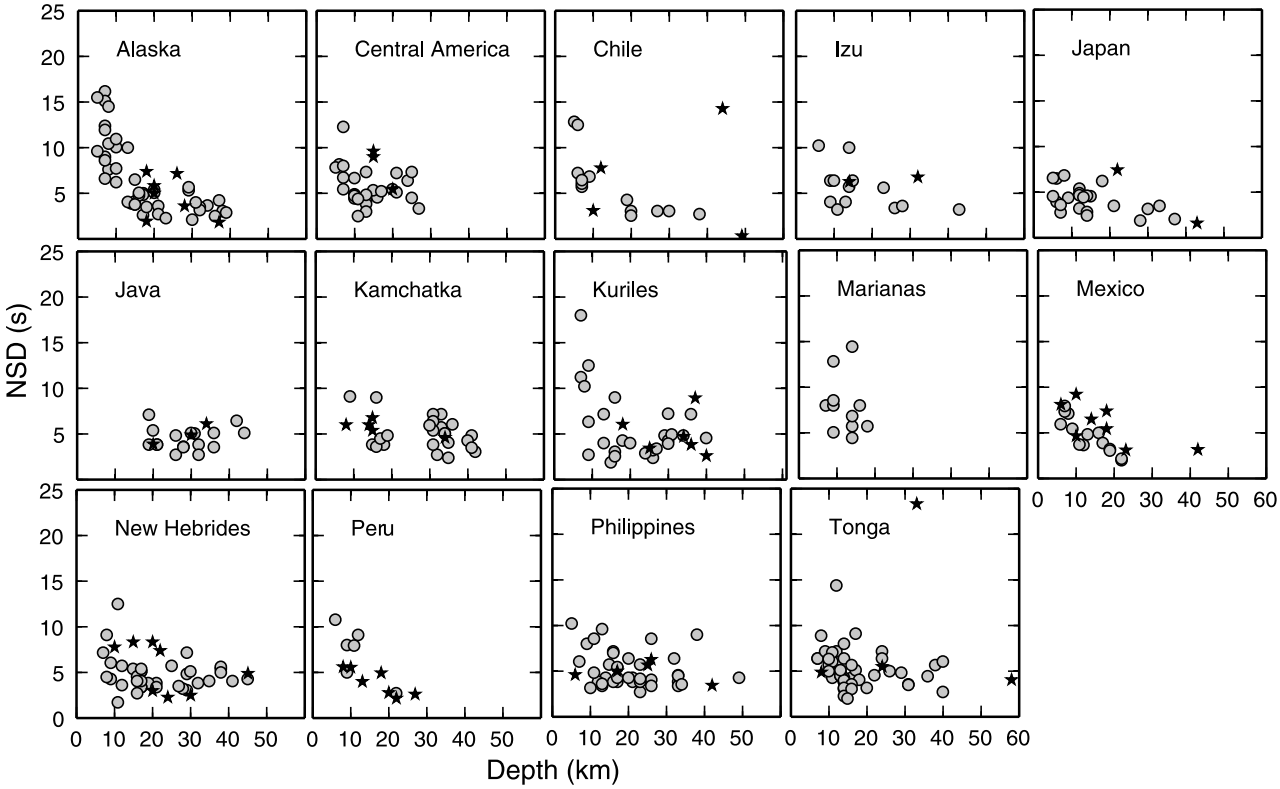

Figure 4. Normalized source duration as a function of centroid depth for the regional earthquake data sets. Stars indicate earthquakes from the MichSeis catalog. Several regions show significant depth variations (i.e., Alaska, Mexico, Peru), while others do not (i.e., Java, Philippines), suggesting possible regional influences on the depth-dependent duration.

thrust earthquakes. A conservative procedure to estimate the radiated energy from the source time functions is to replace the time functions with a symmetric triangle. *Kanamori and Rivera* [2004] present the true energy minimum from displacements of a symmetric parabola form. Our triangle substitution will underestimate the energy for each earthquake [*Tanioka and Ruff*, 1997], as the substitution eliminates any high- frequency features in the time function which can add significant energy [*Vassiliou and Kanamori*, 1982]. However, it does provide a consistent measurement for the entire data set along with allowing for comparison with earlier studies [*Tanioka and Ruff*, 1997].

[24] We replace the source time function with a symmetric triangle of duration d and maximum moment rate m (Figure 5), using the duration and the peak moment rate determined from the source time function shape. Using these parameters, radiated energy E is

$$E = k\frac{m^2}{2d} \tag{1}$$

where

$$k = 8\left(\frac{1}{15\pi\rho\alpha^5} + \frac{1}{10\pi\rho\beta^5}\right) \tag{2}$$

is a constant that depends on properties of the source region. We use a constant value for k, which is a possible source of error in the energy estimates. We may underestimate any depth trend if velocities in the shallowest part of the subduction zone are low. Because we want to identify any regional or depth variations in energy for the earthquakes in the catalog, it is useful to use the energy-moment ratio (E/M_o) instead of the radiated energy. This removes the trend of increasing energy with increasing seismic moment. For a symmetric triangle, the moment M_o is

$$M_o = \frac{md}{2} \tag{3}$$

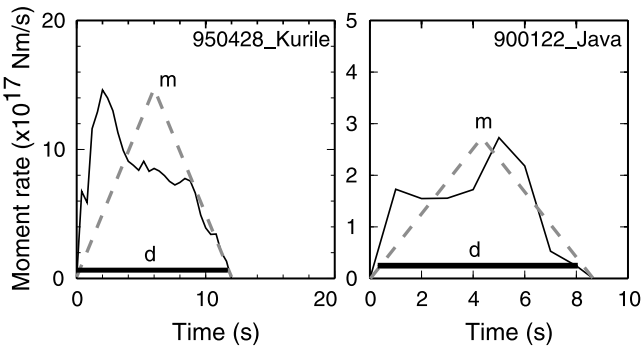

Figure 5. Radiated energy calculation from source time functions. Actual time function is solid line, symmetric triangle representation is dashed line. Duration (d) and maximum moment rate (m) is also shown for both events.

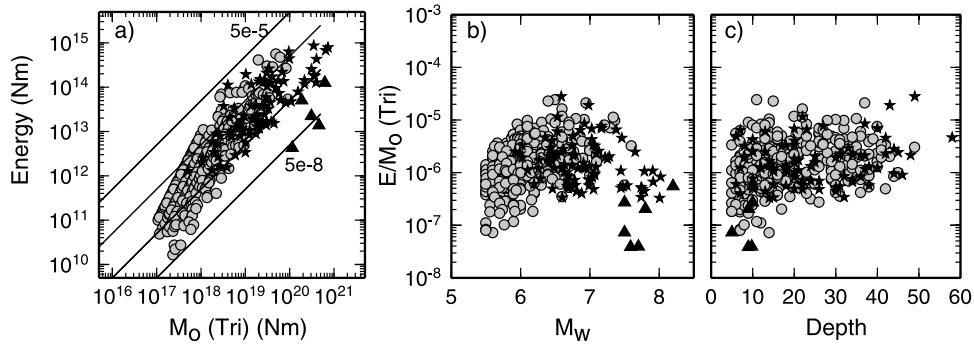

Figure 6. Energy and moment determined using symmetric triangle representation. Stars indicate earthquakes from the MichSeis catalog, and triangles represent values estimated from published source time functions for tsunami earthquakes (see text). (a) Energy as a function of moment, with lines of constant E/M_o shown. Significant scatter apparent, with an average E/M_o of 2.5×10^{-6}. Tsunami earthquakes plot lower. (b) E/M_o as a function of M_w, with tsunami earthquakes falling outside overall population. (c) E/M_o as a function of depth, with little depth trend other than some anomalously low values at the shallowest depths.

giving

$$\frac{E}{M_o} = k\frac{m}{d^2} \tag{4}$$

For our estimates, we use k = 0.0115 $s^3/10^{20}$ N m, valid for shallow crustal earthquakes [*Tanioka and Ruff*, 1997]. Using earthquakes in the MichSeis catalog from 1994 to 1996, *Tanioka and Ruff* [1997] suggest that an E/M_o of 5×10^{-6} provides the best characterization of the observed durations and maximum moment rates with a factor of 10 scatter. This average value for E/M_o encompasses earthquakes from many tectonic environments with a variety of mechanisms, not solely shallow subduction interplate thrust earthquakes.

[25] Energy and moment determined using the symmetric triangle substitution for all source time functions in the combined catalog are compared to the seismic moment, moment magnitude, and depth in Figure 6. Seismic moments determined from the triangle estimates are generally lower than the Harvard CMT catalog values, with some scatter. A comparison of the energy vs moment suggests an average of 2.5×10^{-6} for this shallow subduction zone catalog (Figure 6a), lower than estimated from *Tanioka and Ruff* [1997] using the same method for the entire MichSeis catalog to 1996. Inclusion of all available earthquakes (including intraplate deep and crustal events) by *Tanioka and Ruff* [1997] may account for the differences in average E/M_o estimates. Other studies also suggest a possible mechanism dependence on E/M_o [*Choy and Boatwright*, 1995; *Pérez-Campos and Beroza*, 2001] with strike-slip earthquakes having higher E/M_o than dip-slip earthquakes.

[26] We also estimate radiated seismic energy for tsunami earthquakes for which source time functions have been published. Six historic tsunami earthquakes believed to be associated with faulting rather than submarine slumps have been well studied with information on moment release history: 1946 Alaska [*Johnson and Satake*, 1997], 1960 Peru [*Pelayo and Wiens*, 1990], 1963 and 1975 Kurile [*Pelayo and Wiens*, 1992], 1992 Nicaragua [*Ihmlé*, 1996], 1996 Peru [*Ihmlé et al.*, 1998]. Our estimates of the radiated energy for the tsunami earthquakes use the duration and maximum moment rate from these published time functions (Figure 6).

[27] Comparison of the energy estimates using the simple triangle representation show interesting patterns. First, there is considerable scatter in the estimates. Earthquakes from the MichSeis catalog are similar in value and degree of scatter to our deconvolution results. The tsunami earthquakes clearly stand out from the rest of the shallow subduction zone earthquakes in the combined catalog. The E/M_o of the tsunami events are much lower than for comparably large earthquakes in the catalog, compatible with the results of *Newman and Okal* [1998]. There is not a strong trend in E/M_o with depth, however, the significant scatter may mask a weak trend. The lowest energy estimates are found for events shallower than 15 km. For a simple triangle shape, energy is related to M_o^2/d^3, so it is somewhat surprising that the longer-duration events do not have even lower energy estimates. This lack of a strong trend suggests that extra energy is released as duration increases. One possible way to accomplish this would be to add additional high frequency features within the source time function of the anomalously long-duration earthquakes. Section 4.2 describes energy calculations using the actual source time function shape rather than the simple triangle substitution.

4.2. Shape of Full Source Time Function

[28] Using the full source time function shape to estimate radiated energy involves squaring and integrating the derivative of the source time function. This method will produce higher estimates of energy due to the presence of any high- frequency features in the time function, but is, of course, more dependent on the accuracy of the deconvolved time functions. Following *Vassiliou and Kanamori* [1982], we estimate the energy using

$$E = \left[\frac{1}{15\pi\rho\alpha^5} + \frac{1}{10\pi\rho\beta^5}\right] M_o{}^2 \int \dot{T}^2 \tag{5}$$

where $\dot{T}$ is the moment rate function scaled to unit area. We use density of $\rho = 2.8$ g/cm^3, P wave velocity $\alpha = 6.0$ km/s, and S wave velocity $\beta = \alpha/\sqrt{3}$ for all the calculations.

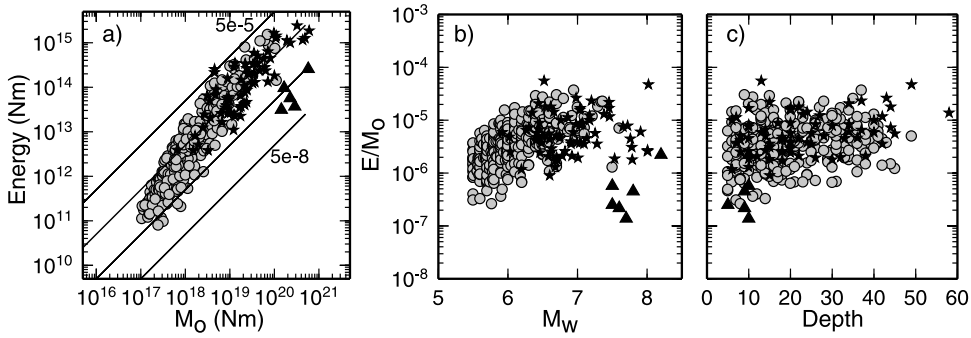

Figure 7. Energy and moment determined using full source time function shape. Stars indicate earthquakes from the MichSeis catalog, and triangles represent values estimated from published source time functions for tsunami earthquakes. (a) Energy as a function of moment, with lines of constant E/M_o shown. Significant scatter is apparent, with an average E/M_o of 5.6×10^{-6}, higher than the triangle estimates. (b) E/M_o as a function of M_w, with tsunami earthquakes falling outside overall population. (c) E/M_o as a function of depth, with very little depth trend observed.

[29] We calculate the energy integrating over the duration of the source time function as defined above (the same as used in the triangle substitution) (Figure 7). As expected, the energy calculated using this method is larger due to the inclusion of higher frequency features of the time function shapes. In fact, the primary difference between these estimates and the triangle representation estimates is a shift to higher energy (Figure 7a) and higher E/M_o (Figures 7b and 7c). A comparison of the energy, moments, and E/M_o estimates from each method are shown in Figure 8. Seismic moment is not significantly different between the 2 methods (Figure 8a), however, for almost every earthquake, the energy calculated using the full source time function shape is larger than the energy calculated with the triangle representation (Figure 8b). Thus E/M_o estimates from the full time function shape calculations are predominantly larger than for the triangle substitution method because of the larger energy values (Figure 8c).

[30] The average E/M_o for our data set is 5.6×10^{-6}. Low values of E/M_o for smaller magnitude events may reflect underestimation of energy for these events. Other studies have estimated radiated energy using a variety of methods: *Kikuchi and Fukao* [1988] find an average E/M_o of 5.0×10^{-6} for large earthquakes, compatible with our result, while *Choy and Boatwright* [1995] find a global average of 1.6×10^{-5}, significantly higher than our estimates. The subset of oceanic subduction zone earthquakes analyzed by *Choy and Boatwright* [1995] has an average of 9.7×10^{-6}, a better value for comparison, as their studies show order of magnitude differences in E/M_o for strike-slip events than for dip-slip events [*Choy and Boatwright*, 1995; *Pérez-Campos and Beroza*, 2001]. *Newman and Okal* [1998] find a global average of 1.05×10^{-5} excluding tsunami earthquakes and 8.7×10^{-6} if three recent tsunami earthquakes are included. *Pérez-Campos and Beroza* [2001] find E/M_o of 8.3×10^{-6} for reverse faulting earthquakes.

[31] Comparison of individual event estimates also show that our estimates are lower than other studies. Comparisons between common events in our data set and the NEIC are provided in the auxiliary material[1]. In general, our energy estimates are a factor of 2 lower than NEIC estimates. This same factor of 2 difference is seen in comparisons with common events in the catalog of *Choy and Boatwright* [1995]. Estimates from *Okal and Newman* [2001] for two events in Java (9 December 1996 and 17 March 1997) and one event in Central America (28 April 1990) are roughly 7 times larger than our estimates. One Mexican earthquake (15 July 1996) from *Pérez-Campos et al.* [2003] has an energy estimate ~6 times larger than our estimate. Eight earthquakes from *Venkataraman and Kanamori* [2004b] included in our data set are between 2 and 7 times larger. There comparisons with other studies suggest that our estimates could be low by factors of 2–7.

[32] We also calculate energy estimates for the tsunami earthquakes using the full time functions (Figure 7). These events are again outliers from the rest of the shallow earthquakes. *Newman and Okal* [1998] provide estimates of E/M_o for tsunami earthquakes, two of which are included in our estimates from the tsunami earthquake time functions. We estimate E/M_o of 1.7×10^{-7} and 5.7×10^{-7} for the 1992 Nicaragua and 1996 Peru tsunami earthquakes. *Newman and Okal* [1998] estimate E/M_o of 5×10^{-7} and 1.15×10^{-6} for the Nicaragua and Peru events, a factor 2–3 times larger than our estimates from the source time functions.

[33] Similar to the results using the triangle representation, a comparison of E/M_o with depth does not show a pronounced trend, other than the lower values of some of the shallowest events, including tsunami earthquakes (Figure 7). A comparison of E/M_o with duration shows no distinct trend, suggesting E/M_o is relatively constant as a function of duration (Figure 9a) [*Tanioka and Ruff*, 1997]. There is a subset of earthquakes that have particularly low E/M_o values, and these events, like the tsunami earthquakes, occur at $\leq$15 km depth (Figure 9b). Because of the high scatter in these estimates, it is useful to separate the earthquakes into regional subsets for comparison (Figure 10). Weak trends of increasing E/M_o with depth in certain regions, such as Alaska, Chile, Japan, Peru, Tonga, and Mexico can be observed. There are regional variations in the average E/M_o as well. Attempts to compare regional averages of E/M_o with estimates from other studies lead to the commonly observed feature that the

[1]Auxiliary material is available at ftp://ftp.agu.org/apend/jb/2004JB003039.

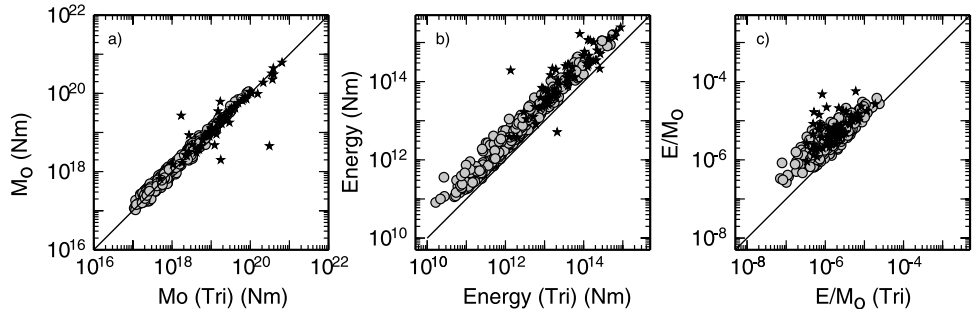

Figure 8. Energy and moment comparison for each calculation method. (a) Moment estimates from full source time function calculation (M_o) compared to triangle estimates (M_o Tri) showing consistent estimates between the two methods. (b) Energy calculated using the full time function shape is consistently higher than energy estimated with the triangle method. (c) Higher E/M_o for the full source time function calculations is a result of higher calculated energy.

teleseismic estimates are lower than the regional estimates. For example, using shallow earthquakes in the Mexican subduction zone we find average E/M_o of 5.7×10^{-6}, while *Singh and Ordaz* [1994] find median E/M_o values of 7.1×10^{-5} using local acceleration data. Loss of high- frequency energy in the teleseismic source time functions may be responsible.

4.3. Source Time Function Complexity

[34] We find rather muted trends between E/M_o and depth in our estimates, and stronger patterns in duration versus depth. High frequency features in the source time function for the longer duration events may account for the muted trends between E/M_o and depth. We characterize the source time function complexity in order to examine whether there is any depth dependence in the relative complexity of the source time functions.

[35] One method of parameterizing source time function complexity is to count the number of peaks in the time function. Higher numbers of peaks (defined as points where the moment rate value is higher than adjacent points) would indicate a more complex or jagged time function. The number of peaks is normalized by the source time function duration however, because simply counting the number of peaks shows a significant positive correlation with longer duration. Tsunami event source time functions are also included in this analysis, and these show a much "simpler" (lower normalized peaks) than the rest of the data set, expected because of their smoother character.

[36] Comparison of normalized peaks with depth (Figure 11) do show greater range in normalized peaks at shallow depth, however it is not clear from the comparison with normalized source duration that the longer normalized duration events have larger normalized peak values (or higher complexity). In fact, the largest range of normalized peak values occurs for the shorter-duration events. This parameterization of source time function complexity is likely not the ideal description of complexity. Time functions with very small roughness in moment rate can lead to large numbers of peaks, but visually would not be classified as a "complex" source time function.

[37] Another way to parameterize source time function complexity is to compare the energy estimates from the triangle substitution with those calculated with the full time function shape. We characterize this difference by the energy ratio

$$E_{\text{ratio}} = \frac{E_{\text{fullSTF}}}{E_{\text{triangle}}} \tag{6}$$

If the time function was sufficiently similar to a triangle, the ratio would be close to 1. An E_{ratio} significantly greater than 1 suggests an increased complexity of the full time function shape away from a simple triangle shape (Figure 12). This parameter is larger for the longer normalized duration earthquakes (Figure 12b). In addition, shallow depth earthquakes have a larger range of E_{ratio} (Figure 12c), again suggesting a large range in complexity for these earth-

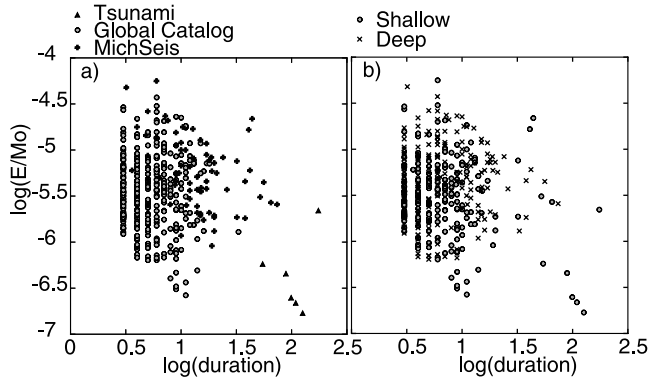

Figure 9. E/M_o compared with duration. (a) Log (E/M_o) as a function of log(duration) for each data set. On the basis of these catalogs, it appears that E/M_o is fairly constant with duration, although with considerable scatter. Tsunami earthquakes stand out relative to the other earthquakes because of their long duration and low E/M_o. (b) Log (E/M_o) as a function of log(duration) and depth. Circles indicate earthquakes with depth $\leq$15 km (including tsunami earthquakes), crosses represent earthquakes deeper than 15 km. There is weak depth separation with E/M_o, as a subset of earthquakes at shallow depth have the lowest E/M_o ratios, similar to the tsunami earthquake values.

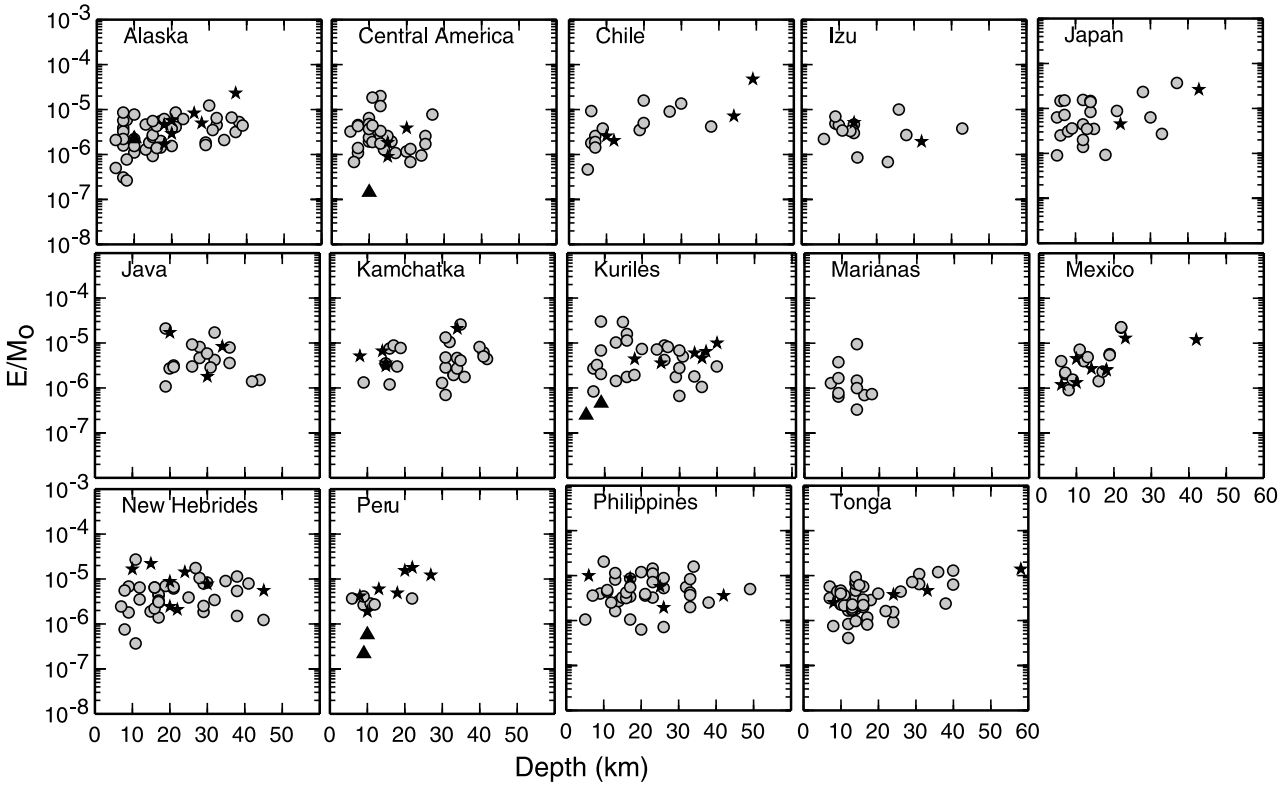

Figure 10. Regional subsets of E/M_o compared with centroid depth. E/M_o is calculated using the full time function shape. Some regions have a depth trend, such as Alaska, Mexico, Peru, and Chile, especially when the MichSeis data are considered.

quakes, which can explain the weakness of any global trend in E/M_o with depth.

5. Discussion

[38] There is significant evidence that earthquake rupture behavior varies both laterally and down dip in shallow subduction zones. Our catalog of source time functions suggests substantial variations in duration and complexity for these earthquakes, particularly at the shallowest seismogenic zone depths. Complexity of earthquake rupture may be related to variations or complexities within the shallow fault zone structure. Fault zone complexities can influence not only the behavior of typical shallow seismicity, but may also influence the generation of tsunami earthquakes [*Bilek and Lay*, 2002]. Here we briefly discuss several ways that complexity may arise in the shallow subduction environment and thus in the shallow earthquake rupture processes. However, this is not an exhaustive discussion of possibilities, as the complex shallow subduction zone environment is a region of continued research and exploration.

5.1. Fluid Processes

[39] Fluids are introduced into subduction zone systems in several ways, and with the potential for large volumes of fluids being present, it is likely that fluids may influence

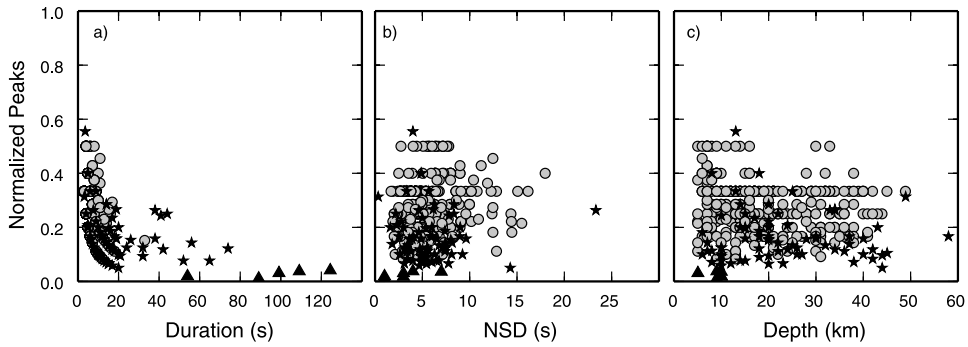

Figure 11. Source time function complexity parameterized by normalized number of peaks. (a) Normalized peaks as a function of duration. (b) Normalized peaks as a function of normalized duration. (c) Normalized peaks as a function of depth. Trends in this parameter are hard to distinguish and may be complicated by the peak definition.

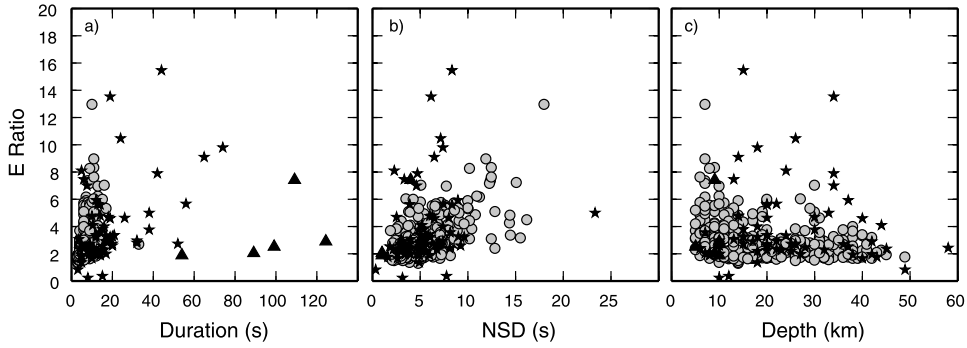

Figure 12. Source time function complexity parameterized by E_{ratio}. (a) E_{ratio} as a function of duration. (b) E_{ratio} as a function of normalized duration. longer-duration earthquakes have large range of E_{ratio}, with some of the highest values of E_{ratio}, suggesting more complexity in the source time functions for the longer-duration events. (c) E_{ratio} as a function of depth. Shallow earthquakes have large range of E_{ratio}, again suggesting higher complexity for shallow time functions.

earthquake rupture behavior. Two main contributing processes to introduce fluids into subduction zones are sediment consolidation and dewatering [*Moore and Vrolijk*, 1992], which work to decrease material porosities [*Bray and Karig*, 1985]. Variation in porosities can affect fluid migration paths that can vary spatially and temporally [*Peacock*, 1990; *Carson and Screaton*, 1998; *Saffer and Bekins*, 1999].

[40] Variability in fluids within the fault zone can influence earthquake rupture, as evidenced by earthquakes on the San Andreas Fault near Parkfield [*Eberhart-Phillips and Michael*, 1993; *Johnson and McEvilly*, 1995] and numerical models of earthquake rupture on subduction zone faults [*Taylor and Rice*, 1998]. Results from numerical modeling of an undrained fault predict earthquake rupture at depth to slow and stop at shallow depth and to produce slip with considerably slower rupture velocity near the surface in days after the event [*Taylor and Rice*, 1998]. This result has bearing on the occurrence of slow creep events, with significant postseismic moment release, and possibly can contribute to long-duration shallow events seen in our global data set.

5.2. Sediment Variations

[41] Variations in sediment thickness, mineralogy, and mineralogic reactions can influence fault behavior and seismicity as evidenced by laboratory experiments and seismic observations. *Marone and Scholz* [1988] describe stable to unstable sliding in the presence of unconsolidated gouge material in strike-slip fault zones, with *Byrne et al.* [1988] suggesting a similar mechanism for subduction zone seismicity limits. Sediment thickness may also influence thermal structure and seismicity limits as well as earthquake rupture variations [*Oleskevich et al.*, 1999; *Tanioka et al.*, 1996; *Ruff*, 1989]. Mineralogy of the subducted sediment also influences seismicity and fault behavior, with mineral porosity variations being important [*Gregory*, 1976; *Wang*, 1980; *Vrolijk*, 1990; *Hyndman and Wang*, 1993; *Zhang et al.*, 1993] as well as mineral reactions which can alter mineral fabrics and thus fault strength and strain localization [*Byrne*, 1998; *Vrolijk and van der Pluijm*, 1999; *Moore and Saffer*, 2001; *Saffer and Marone*, 2003]. Unfortunately, detailed catalogs of sediment variations are not yet available for each subduction zone for comparison with earthquake rupture behavior.

5.3. Variable Incoming Plate Structure

[42] The underthrusting plate structure in many subduction zones show significant diversity in bathymetric features. Fracture zones, horst and graben structures, seamounts, and oceanic ridges subduct in various regions, with likely effects on the mechanical properties [*Cloos*, 1992; *Scholz and Small*, 1997]. This roughness on the incoming plate can influence earthquake rupture behavior as suggested for earthquakes offshore NE Japan. *Tanioka et al.* [1996] suggest lateral variations in earthquake rupture along this margin, with large thrust events in regions of smooth plate contact and tsunami, slow earthquakes in regions of subducting sediment filled grabens. These lateral variations may also impact the character of smaller magnitude earthquakes, as *Bilek* [2001] find some evidence of longer-duration earthquakes in the regions of significant plate roughness. Source time functions for earthquakes in regions of increased heterogeneity of the subducting plate tend to be more complex because of the more complex waveforms for earthquakes in these regions, so values of radiated energy would likely be higher in these regions rather than regions of smooth plate subduction. Energy will also be affected by factors other than this heterogeneity, such as overall stress levels; however, heterogeneity levels at individual subduction zones likely contribute to the scatter seen in our global earthquake parameter catalog.

5.4. Frictional Conditions on the Megathrust

[43] It is clear that many of these processes are interconnected, and it is likely that no single process controls shallow subduction seismicity variations. For example, *Moore and Saffer* [2001] and *Saffer and Marone* [2003] suggest that shallow subduction megathrust zone frictional stability conditions, notably the transition from aseismic (velocity strengthening) to seismic (velocity weakening) behavior, are not controlled by a single process; instead combinations of several other depth- and temperature-dependent processes, such as a variety of diagenetic/low grade metamorphic processes, fluid pressure changes, and slip localization, may dictate friction.

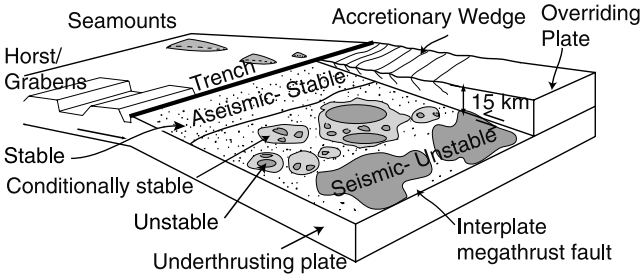

Figure 13. Simplified view of the frictional conditions within the shallow subduction zone environment, modified from *Bilek and Lay* [2002]. Aseismic conditions may exist at the shallowest extent of the fault zone, with laterally variable zones of unstable and conditionally stable frictional regimes at depth. Patches of unstable material within conditionally stable zones may be due to variations in bathymetry, sediment or fluid conditions. Heterogeneity in these frictional conditions may give rise to the variations in rupture duration and radiated energy described for shallow subduction zone earthquakes.

Pacheco et al. [1993] suggest stability variations may be caused by differences in sediment composition, plate roughness, and/or fluid pressures in the fault zone. Given these possible controls on the friction conditions, it is likely that there will be significant lateral variations in stability [*Pacheco et al.*, 1993].

[44] In the progression from stable to unstable friction conditions in the shallow subduction zone, there appears to be a transition into a conditionally stable region. This region usually behaves aseismically, but may fail seismically if loaded at a high strain rate [*Scholz*, 1990, 1998]. This conditionally stable zone may contain sedimentary materials with lower strength. Although earthquakes nucleate in unstable conditions, slip may propagate into the conditionally stable regions on the fault, possibly with slower rupture velocities than for slip in unstable regions.

[45] A simplified form of the shallow subduction interface in terms of these friction conditions is shown in Figure 13. An aseismic zone may exist at the shallowest extent beneath sediments in an accretionary wedge. Within the transition from stable to unstable conditions, the megathrust zone enters a conditionally stable regime, a heterogeneous region including portions of unstable friction due to lateral variations in pore pressures, subducting sediment and bathymetric features. Earthquakes, including tsunami earthquakes, which nucleate in the unstable portions of this region and propagate into conditionally stable materials may have slower rupture velocities, longer durations, and increased slip heterogeneity (added source time function complexity) [*Bilek and Lay*, 2002]. These shallow earthquakes may have the observed behavior, with longer rupture durations and increased source time function complexity that gives higher E/M_o ratios than expected for the source duration, compared to deeper earthquakes which rupture in a more uniform area of unstable friction conditions expected deeper along the fault.

[46] If these interconnected processes influence initiation of seismicity and seismic coupling in subduction zones, it is likely that combinations of processes will also affect earthquake rupture behavior along the subduction zone plate interface. Further work is needed in order to more accurately pinpoint which processes are most important for controlling frictional conditions. *Moore and Saffer* [2001] examined the roles of several processes affecting the updip seismic limit in southwest Japan because of the wealth of data available about the structure and materials of that particular subduction zone. However, comparable information is needed for other subduction zones around the Pacific in order to fully describe which processes are most important in influencing earthquake rupture at depth in subduction zones.

6. Conclusions

[47] Earthquake source time functions for shallow subduction zone thrust earthquakes show patterns suggesting complexity in the shallow seismogenic environment. Rupture duration estimates for 417 events in 14 circum-Pacific subduction zones show depth dependence, with some moment normalized source duration being anomalously long at depths from 0 to 15 km. The radiated seismic energy does not show as much of a global trend with depth as would be expected for simple time functions. Increased time function complexity of the shallower, long-duration earthquakes may explain the weakness of any global trend in E/M_o with depth. Increased source time function complexity and anomalous earthquake rupture duration behavior in the shallow subduction zone environment could be produced by a variety of features and processes, such as fluid flow, thermal structure, and sediment deformation mechanisms. However, combinations of processes are likely to interact to influence earthquake rupture. Additional data concerning the structure and materials of the various subduction zone is needed in order to quantify the true influences of these processes on earthquake rupture.

[48] **Acknowledgments.** We thank the two anonymous reviewers and Associate Editor Ed Garnero for their suggestions to improve the manuscript. Earthquake data were obtained from the IRIS Data Management Center for stations of the Global Seismic Network and Federation of Digital Seismic Networks [*Butler et al.*, 2004]. This work was partially supported by NSF grant EAR0125595 (T.L.) and a Turner Postdoctoral Fellowship at the University of Michigan (S.B.). Contribution 471 of the Center for Study of Imaging and Dynamics of the Earth at UCSC.

References

Bilek, S. (2001), *Earthquake rupture processes in circum-Pacific subduction zones*, Ph.D. thesis, Univ. of Calif., Santa Cruz.

Bilek, S., and T. Lay (1999), Rigidity variations with depth along interplate megathrust faults in subduction zones, *Nature*, *400*, 443–446.

Bilek, S., and T. Lay (2000), Depth dependent rupture properties in circum-Pacific subduction zones, in *GeoComplexity and the Physics of Earthquakes*, *Geophys. Monogr. Ser.*, vol. 20, edited by J. Rundle, D. Turcotte, and W. Klein, pp. 165–186, AGU, Washington, D. C.

Bilek, S. L., and T. Lay (2002), Tsunami earthquakes possibly widespread manifestations of frictional conditional stability, *Geophys. Res. Lett.*, *29*(14), 1673, doi:10.1029/2002GL015215.

Bos, A., G. Nolet, A. Rubin, H. Houston, and J. Vidale (1998), Duration of deep earthquakes determined by stacking of Global Seismograph Network seismograms, *J. Geophys. Res.*, *103*, 21,059–21,065.

Bray, C., and D. Karig (1985), Porosity of sediments in accretionary prisms and some implications for dewatering processes, *J. Geophys. Res.*, *90*, 768–778.

Butler, R., et al. (2004), The Global Seismographic Network surpasses its design goal, *Eos Trans. AGU*, *85*(23), 225.

Byrne, D., D. Davis, and L. Sykes (1988), Loci and maximum size of thrust earthquakes and the mechanics of the shallow region of subduction zones, *Tectonics*, *7*, 833–857.

Byrne, T. (1998), Seismicity, slate belts, and coupling along convergent plate boundaries, *Eos Trans. AGU*, *79*, , West. Pac. Meet., W114.
Campus, P., and S. Das (2000), Comparison of the rupture and radiation characteristics of intermediate and deep earthquakes, *J. Geophys. Res.*, *105*, 6177–6189.
Carson, B., and E. Screaton (1998), Fluid flow in accretionary prisms: Evidence for focused, time variable discharge, *Rev. Geophys.*, *36*, 329–351.
Choy, G., and J. Boatwright (1995), Global patterns of radiated seismic energy and apparent stress, *J. Geophys. Res.*, *100*, 18,205–18,228.
Christensen, D., and L. Ruff (1985), Analysis of the trade-off between hypocentral depth and source time function, *Bull. Seismol. Soc. Am.*, *75*, 1637–1656.
Cloos, M. (1992), Thrust-type subduction zone earthquakes and seamount asperities: A physical model for seismic rupture, *Geology*, *20*, 601–604.
Dragert, H., K. Wang, and T. James (2001), A silent slip event on the deeper Cascadia subduction interface, *Science*, *292*, 1525–1528.
Dziewonski, A., and D. Anderson (1981), Preliminary reference earth model, *Phys. Earth Planet. Inter.*, *25*, 297–356.
Eberhart-Phillips, D., and A. Michael (1993), Three-dimensional velocity structure, seismicity, and fault structure in the Parkfield region, central California, *J. Geophys. Res.*, *98*, 15,735–15,738.
Ekström, G., and E. Engdahl (1989), Earthquake source parameters and stress distribution in the Adak Island region of the central Aleutian Islands, *J. Geophys. Res.*, *94*, 15,499–15,519.
Fukao, Y. (1979), Tsunami earthquakes and subduction processes near deep-sea trenches, *J. Geophys. Res.*, *84*, 2303–2314.
Gregory, A. (1976), Fluid saturation effects on dynamic elastic properties of sedimentary rocks, *Geophysics*, *41*, 895–921.
Heki, K., and Y. Tamura (1997), Short term afterslip in the 1994 Sanriku-Haruka-Oki earthquake, *Geophys. Res. Lett.*, *24*, 3285–3288.
Heki, K., S. Miyazaki, and H. Tsuji (1997), Silent fault slip following an interplate thrust earthquake at the Japan trench, *Nature*, *386*, 595–598.
Houston, H. (2001), Influence of depth, focal mechanism, and tectonic setting on the shape and duration of earthquake source time functions, *J. Geophys. Res.*, *106*, 11,137–11,150.
Houston, H., H. Benz, and J. Vidale (1998), Time functions of deep earthquakes from broadband and short period stacks, *J. Geophys. Res.*, *103*, 29,895–29,913.
Hyndman, R., and K. Wang (1993), Thermal constraints on the zone of major thrust earthquake failure: The Cascadia subduction zone, *J. Geophys. Res.*, *98*, 2039–2060.
Ihmlé, P. (1996), Frequency-dependent relocation of the 1992 Nicaragua slow earthquake: An empirical greens function approach, *Geophys. J. Int.*, *125*, 75–85.
Ihmlé, P., J.-M. Gomez, P. Heinrich, and S. Guibourg (1998), The 1996 Peru tsunamigenic earthquake: Broadband source process, *Geophys. Res. Lett.*, *25*, 2691–2694.
Jarrard, R. (1986), Relation among subduction parameters, *Rev. Geophys.*, *24*, 217–284.
Johnson, J., and K. Satake (1997), Estimation of seismic moment and slip distribution of the April 1, 1946, Aleutian tsunami earthquake, *J. Geophys. Res.*, *102*, 11,765–11,779.
Johnson, P., and T. McEvilly (1995), Parkfield seismicity: Fluid driven?, *J. Geophys. Res.*, *100*, 12,937–12,950.
Kanamori, H. (1972), Mechanism of tsunami earthquakes, *Phys. Earth Planet. Inter.*, *6*, 246–259.
Kanamori, H. (1994), Mechanics of earthquakes, *Annu. Rev. Earth Planet. Sci.*, *22*, 207–237.
Kanamori, H., and D. Anderson (1975), Theoretical basis of some empirical relations in seismology, *Bull. Seismol. Soc. Am.*, *65*, 1073–1095.
Kanamori, H., and M. Kikuchi (1993), The 1992 Nicaragua earthquake: A slow tsunami earthquake associated with subducted sediments, *Nature*, *361*, 714–716.
Kanamori, H., and L. Rivera (2004), Static and dynamic scaling relations for earthquakes and their implications for rupture speed and stress drop, *Bull. Seismol. Soc. Am.*, *94*, 314–319.
Kawasaki, I., Y. Asai, Y. Tamura, T. Sagiya, N. Mikami, Y. Okada, M. Sakata, and M. Kasahara (1995), The 1992 Sanriku-Oki, Japan, ultra-slow earthquake, *J. Phys. Earth*, *43*, 105–116.
Kikuchi, M., and Y. Fukao (1988), Seismic wave energy inferred from long-period body wave inversion, *Bull. Seismol. Soc. Am.*, *78*, 1707–1724.
Lay, T., H. Kanamori, and L. Ruff (1982), The asperity model and the nature of large subduction zone earthquakes, *Earthquake Predict. Res.*, *1*, 3–71.
Lowry, A., K. Larson, V. Kostoglodov, and R. Bilham (2001), Transient fault slip in Guerrero, southern Mexico, *Geophys. Res. Lett.*, *28*, 3753–3756.
Marone, C., and C. Scholz (1988), The depth of seismic faulting and the upper transition from stable to unstable slip regimes, *Geophys. Res. Lett.*, *6*, 621–624.
Mayeda, K., and W. Walter (1996), Moment, energy, stress drop, and source spectra of western United States earthquakes from regional coda envelopes, *J. Geophys. Res.*, *101*, 11,195–11,208.
McGarr, A. (1999), On relating apparent stress to the stress causing earthquake fault slip, *J. Geophys. Res.*, *104*, 3003–3011.
McGuire, J., and P. Segall (2003), Imaging of aseismic fault slip transients recorded by dense geodetic networks, *Geophys. J. Int.*, *155*, 778–788.
Melbourne, T., F. Webb, J. Stock, and C. Reigber (2002), Rapid postseismic transients in subduction zones from continuous gps, *J. Geophys. Res.*, *107*(10), 2241, doi:10.1029/2001JB000555.
Miller, M., T. Melbourne, D. Johnson, and W. Sumner (2002), Periodic slow earthquakes from the Cascadia subduction zone, *Science*, *295*, 2423.
Moore, J., and D. Saffer (2001), The updip limit of the seismogenic zone beneath the accretionary prism of southwest Japan: An effect of diagenetic to low-grade metamorphic processes and increasing effective stress, *Geology*, *29*, 183–186.
Moore, J., and P. Vrolijk (1992), Fluids in accretionary prisms, *Rev. Geophys.*, *30*, 113–135.
Newman, A., and E. Okal (1998), Teleseismic estimates of radiated seismic energy: The E/M_o discriminant for tsunami earthquakes, *J. Geophys. Res.*, *103*, 26,885–26,898.
Okal, E. (1988), Seismic parameters controlling far-field tsunami amplitudes: A review, *Nat. Hazards*, *1*, 67–96.
Okal, E., and A. Newman (2001), Tsunami earthquakes: The quest for a regional signal, *Phys. Earth Planet. Inter.*, *124*, 45–70.
Oleskevich, D., R. Hyndman, and K. Wang (1999), The updip and downdip limits to great subduction earthquakes: Thermal and structural models of Cascadia, south Alaska, SW Japan, and Chile, *J. Geophys. Res.*, *104*, 14,965–14,991.
Pacheco, J., L. Sykes, and C. Scholz (1993), Nature of seismic coupling along simple plate boundaries of the subduction type, *J. Geophys. Res.*, *98*, 14,133–14,159.
Peacock, S. (1990), Fluid processes in subduction zones, *Science*, *248*, 329–337.
Pelayo, A., and D. Wiens (1990), The November 20, 1960 Peru tsunami earthquake: Source mechanism of a slow earthquake, *Geophys. Res. Lett.*, *17*, 661–664.
Pelayo, A., and D. Wiens (1992), Tsunami earthquakes: Slow thrust-faulting events in the accretionary wedge, *J. Geophys. Res.*, *97*, 15,321–15,337.
Pérez-Campos, X., and G. Beroza (2001), An apparent mechanism dependence of radiated seismic energy, *J. Geophys. Res.*, *106*, 11,127–11,136.
Pérez-Campos, X., S. Singh, and G. Beroza (2003), Reconciling teleseismic and regional estimates of seismic energy, *Bull. Seismol. Soc. Am.*, *93*, 2123–2130.
Peterson, E., and T. Seno (1984), Factors affecting seismic moment release rates in subduction zones, *J. Geophys. Res.*, *89*, 10,233–10,248.
Polet, J., and H. Kanamori (2000), Shallow subduction zone earthquakes and their tsunamigenic potential, *Geophys. J. Int.*, *142*, 684–702.
Rea, D., and L. Ruff (1996), Composition and mass flux of sediment entering the world's subduction zones: Implications for global sediment budgets, great earthquakes, and volcanism, *Earth Planet. Sci. Lett.*, *140*, 1–12.
Ruff, L. (1989), Do trench sediments affect great earthquake occurrence in subduction zones?, *Pure Appl. Geophys.*, *129*, 263–282.
Ruff, L., and H. Kanamori (1980), Seismicity and the subduction process, *Phys. Earth Planet. Inter.*, *23*, 240–252.
Ruff, L., and H. Kanamori (1983), The rupture process and asperity distribution of three great earthquakes from long period diffracted *p*-waves, *Phys. Earth Planet. Inter.*, *31*, 202–230.
Ruff, L., and A. Miller (1994), Rupture process of large earthquakes in the northern Mexico subduction zone, *Pure Appl. Geophys.*, *142*, 101–171.
Saffer, D., and B. Bekins (1999), Fluid budgets at convergent plate margins: Implications for the extent and duration of fault zone dilation, *Geology*, *27*, 1095–1098.
Saffer, D., and C. Marone (2003), Comparison of smectite- and illite-rich gouge frictional properties: Application to the updip limit of the seismogenic zone along subduction megathrusts, *Earth Planet. Sci. Lett.*, *215*, 219–235.
Satake, K. (1994), Mechanism of the 1992 Nicaragua tsunami earthquake, *Geophys. Res. Lett.*, *21*, 2519–2522.
Satake, K., and Y. Tanioka (1999), Sources of tsunami and tsunamigenic earthquakes in subduction zones, *Pure Appl. Geophys.*, *154*, 467–483.
Scholz, C. (1990), *The Mechanics of Earthquakes and Faulting*, 449 pp., Cambridge Univ. Press, New York.
Scholz, C. (1998), Earthquakes and friction laws, *Nature*, *391*, 37–42.

Scholz, C., and C. Small (1997), The effect of seamount subduction on seismic coupling, *Geology*, *25*, 487–490.
Seno, T. (2002), Tsunami earthquakes as transient phenomena, *Geophys. Res. Lett.*, *29*(10), 1419, doi:10.1029/2002GL014868.
Singh, S., and M. Ordaz (1994), Seismic energy release in Mexican subduction zone earthquakes, *Bull. Seismol. Soc. Am.*, *84*, 1533–1550.
Tanioka, Y., and L. Ruff (1997), Source time functions, *Seismol. Res. Lett.*, *68*, 386–397.
Tanioka, Y., and K. Satake (1996), Fault parameters of the 1896 Sanriku tsunami earthquake estimated from tsunami numerical modeling, *Geophys. Res. Lett.*, *23*, 1549–1552.
Tanioka, Y., L. Ruff, and K. Satake (1996), What controls the lateral variation of large earthquake occurrence along the Japan trench?, *Island Arc*, *6*, 261–266.
Taylor, M., and J. Rice (1998), Dilatant stabilization of subduction earthquake rupture into the shallow thrust interface, *Eos Trans. AGU*, *79*, Fall Meet. Suppl., F631.
Tichelaar, B., and L. Ruff (1991), Seismic coupling along the Chilean subduction zone, *J. Geophys. Res.*, *96*, 11,997–12,022.
Tichelaar, B., and L. Ruff (1993), Depth of seismic coupling along subduction zones, *J. Geophys. Res.*, *98*, 2017–2037.
Vassiliou, M., and H. Kanamori (1982), The energy release in earthquakes, *Bull. Seismol. Soc. Am.*, *72*, 371–387.
Venkataraman, A., and H. Kanamori (2004a), Effect of directivity on estimates of radiated seismic energy, *J. Geophys. Res.*, *109*, B04301, doi:10.1029/2003JB002548.
Venkataraman, A., and H. Kanamori (2004b), Observational constraints on the fracture energy of subduction zone earthquakes, *J. Geophys. Res.*, *109*, B05302, doi:10.1029/2003JB002549.
Venkataraman, A., L. Rivera, and H. Kanamori (2002), Radiated energy from the 16 October 1999 Hector Mine earthquake: Regional and teleseismic estimates, *Bull. Seismol. Soc. Am.*, *92*, 1256–1265.
Vidale, J., and H. Houston (1993), The depth dependence of earthquake duration and implications for rupture mechanics, *Nature*, *35*, 45–47.
von Huene, R., and D. Scholl (1991), Observations at convergent margins concerning sediment subduction, subduction erosion, and the growth of continental crust, *Rev. Geophys.*, *29*, 279–316.
Vrolijk, P. (1990), On the mechanical role of smectite in subduction zones, *Geology*, *18*, 703–707.
Vrolijk, P., and B. van der Pluijm (1999), Clay gouge, *J. Struct. Geol.*, *21*, 1039–1048.
Wang, C. (1980), Sediment subduction and frictional sliding in a subduction zone, *Geology*, *8*, 530–533.
Winslow, N., and L. Ruff (1999), A hybrid method for calculating the radiated wave energy of deep earthquakes, *Phys. Earth Planet. Inter.*, *115*, 181–190.
Zhang, J., D. Davis, and T.-F. Wong (1993), The brittle-ductile transition in porous sedimentary rocks: Geological implications for accretionary wedge aseismicity, *J. Struct. Geol.*, *15*, 819–830.
Zhang, Z., and S. Schwartz (1992), Depth distribution of moment release in underthrusting earthquakes at subduction zones, *J. Geophys. Res.*, *97*, 537–544.

S. L. Bilek, Department of Earth and Environmental Science, New Mexico Institute of Mining and Technology, Socorro, NM 87801, USA. (sbilek@ees.nmt.edu)
T. Lay, Earth Sciences Department, 1156 High Street, University of California Santa Cruz, Santa Cruz, CA 95064, USA. (tlay@es.ucsc.edu)
L. J. Ruff, Department of Geological Sciences, 425 E. University Ave., University of Michigan, Ann Arbor, MI 48109, USA. (ruff@umich.edu)